Supporting information

# Spectrum-Quantified Morphological Evolution of Enzyme-Protected Silver Nanotriangles by DNA-Guided Postshaping

Junyao Li,[†] Runkun Chen,[‡] Qinghua Zhang,[‡] Jian Zhao,[†] Jianing Chen,[‡] Lin Gu,[‡] Zhaoyin Wang,*[,†] and Zhihui Dai*[,†]

[†]Jiangsu Collaborative Innovation Center of Biomedical Functional Materials and Key Laboratory of Biofunctional Materials of Jiangsu Province, School of Chemistry and Materials Science, Nanjing Normal University, Nanjing 210023, People's Republic of China.

[‡]Beijing National Laboratory for Condensed Matter Physics, Institute of Physics, Chinese Academy of Sciences, Beijing 100190, People's Republic of China.

*Tel./Fax: +86-25-85891051. E-mail: inzo@163.com (Z. Wang); daizhihuii@njnu.edu.cn (Z. Dai).

## List of contents:

# 1. Experimental section and computational method.

## Reagents

Poly(vinylpyrrolidone) (PVP), silver nitrate ($AgNO_3$), trisodium citrate (TSC), hydrogen peroxide 30% aqueous solution ($H_2O_2$), sodium borohydride ($NaBH_4$), sodium chloride (NaCl), ethanol, ethylene glycol (EG), polyethylene glycol (PEG), peroxidase from horseradish (HRP), bovine serum albumin (BSA), pepsin, glycine (Gly), 2'-deoxyadenosine 5'-triphosphate disodium salt solution (dATP), thymidine 5'-triphosphate sodium salt solution (dTTP), 2'-deoxycytidine 5'-triphosphate disodium salt solution (dCTP), 2'-deoxyguanosine 5'-triphosphate sodium salt solution (dGTP), zinc acetate ($Zn(CH_3COO)_2$), and cobalt acetate ($Co(CH_3COO)_2$) were all received from Sigma-Aldrich Co., Ltd. (Shanghai, China). S1 nuclease (S1) was purchased from Promega Corporation. Terminal deoxynucleotidyl transferase (TdT) was purchased from Thermo Fisher Scientific (Shanghai, China). Lambda exonuclease (λ Exo), klenow fragment (K F), Nt.BbvCI were provided by New England Biolabs (NEB) Ltd. (Beijing, China). T4 DNA ligase (T4) was acquired from Takara Biotechnology Co., Ltd. (Dalian, China). Titanic sulfate ($Ti(SO_4)_2$) was purchased from Aladdin Biochemical Technology Co., Ltd. (Shanghai, China). All of the reagents were of analytical grade and were used without further purification. Solutions were prepared with ultrapure water (18.2 MΩ cm) from a Milli-Q purification system (Bedford, MA). Oligonucleotides were obtained and purified with HPLC by Takara Co., Ltd. (Dalian, China). Sequences of all oligonucleotides used in this work are listed as followed.

**Table S1. Sequences of oligonucleotides used in this work.**

| Name | Sequences from 5' to 3' |
|---|---|
| Poly(30A) | AAAAAAAAAAAAAAAAAAAAAAAAAAAAAA |
| Poly(30T) | TTTTTTTTTTTTTTTTTTTTTTTTTTTTTT |
| Poly(30C) | CCCCCCCCCCCCCCCCCCCCCCCCCCCCCC |
| Poly(30G) | GGGGTGGGGGGTGGGGGGTGGGGGGTGGGG |
| Poly(5C) | CCCCC |
| Poly(10C) | CCCCCCCCCC |
| Poly(15C) | CCCCCCCCCCCCCCC |
| Poly(20C) | CCCCCCCCCCCCCCCCCCCC |

| | |
|---|---|
| Poly(25C) | CCCCCCCCCCCCCCCCCCCCCCCCC |
| Poly(35C) | CCCCCCCCCCCCCCCCCCCCCCCCCCCCCCCCCCC |
| Poly(CT) | CTCTCTCTCTCTCTCTCTCTCTCTCTCT |
| Poly(CCT) | CCTCCTCCTCCTCCTCCTCCTCCTCCT |
| Poly(CCCT) | CCCTCCCTCCCTCCCTCCCTCCCTCCCTCC |
| Poly(CCCCT) | CCCCTCCCCTCCCCTCCCCTCCCCTCCCCT |
| Poly(CCCCCT) | CCCCCTCCCCCTCCCCCTCCCCCTCCCCCT |
| Poly(10T) | TTTTTTTTTT |

**Instrumentation**

The transmission electron microscopy (TEM) images, high-resolution transmission electron microscopy (HRTEM) images, selected area electron diffraction (SAED) analysis were characterized using a JEOL JEM-2100F operated at an accelerating voltage of 200 kV. Extinction spectra were measured on a Varian Cary 5000 UV-vis spectrophotometer (Varian, America). The atomic structures (HAADF-STEM images) of the AgNTs were investigated using an ARM-200CF transmission electron microscope operated at 200 kV and equipped with double spherical aberration (Cs) correctors. The scanning electron microscope (SEM) image of HRP was characterized using a JEOL JSM-7600F. The SEM and STEM images of HRP-protected AgNTs were characterized using a JEOL JEM-2800 operated at an accelerating voltage of 200 kV. The X-ray diffraction (XRD) patterns were obtained using a D/max 2500 VL/PC diffractometer (Japan) equipped with graphite monochromatized Cu Kα radiation (λ = 1.54060 Å). The X-ray photoelectron spectroscopy (XPS) was performed on an ESCALAB $Xi^+$ (Thermo Fisher Scientific, America).

**Synthesis of HRP-protected AgNTs.**

The AgNTs were synthesized according to a previous study with slight modifications.[S1] Typically, 145 mL of aqueous solution containing $AgNO_3$ (50 mM, 300 μL), TSC (75 mM, 3 mL), PVP (17.5 mM, 1.2 mL), and $H_2O_2$ (30 wt %, 720 μL) were mixed in a 250 mL flask and allowed to vigorously stir at room temperature for 30 min. $NaBH_4$ solution (100 mM, 1.5 mL) was rapidly added into this mixture, generating pale yellow colloid solution. Afterward, the solution changed gradually from pale yellow to yellow, red, purple, blue, and green, indicating the formation of AgNTs. Then, HRP solution (1 mg/mL, 1.48 mL) was injected into this mixture that was slowly stirred for another 30

min. The resultant HRP-protected AgNTs solutions could be stable in dark (4°C) for at least 4 weeks. To improve the yield of intact AgNTs, different amounts of $H_2O_2$ (0, 180, 360, 540, 720, 900, 1080 uL) and HRP (0, 0.5, 1, 1.5, 2 mg/mL) were tested in synthesizing AgNTs. HRP, BSA, pepsin, and Gly (1 mg/mL, 1.48 mL) were chosen to survey the effect of different biomolecules on AgNTs.

**Determination of residual $H_2O_2$ in as-prepared AgNTs.**

$H_2O_2$ was determined by chromogenic reaction of $Ti(SO_4)_2$. First, $Ti(SO_4)_2$ solution was prepared by dissolving 50 mg of $Ti(SO_4)_2$ into 8.33 mL of $H_2SO_4$, and diluted with ultrapure water to 50 mL. Then, 400 μL $Ti(SO_4)_2$ solution was mixed with 100 μL supernate of as-prepared AgNTs. Sixty min later, absorption spectrum of the solution was recorded to evaluate the residual $H_2O_2$ in as-prepared AgNTs.

**Shaping of HRP-protected AgNTs with DNA.**

DNA-guided postshaping was carried out by mixing poly(30C) (10 μM, 40 μL) with AgNTs solutions (360 μL). After equilibrated at room temperature for 70 min in the dark, the mixture was ready to obtain extinction spectra. To testify the effect of other DNA, poly(30C) was replaced with equal concentration of poly(30A), poly(30T), poly(30G), poly(5C), poly(10C), poly(20C), poly(25C), and poly(35C), respectively. To investigate the effect of dNTP, total amount of base was kept constant by replacing poly(30C) with 40 μL of 300 μM dATP, dTTP, dCTP, and dGTP. To compare the effect of halide ions, 40 μL of 1 mM and 10 mM NaCl were chosen to etch AgNTs. To form mismatched base pairs, 20 μL of 20 μM poly(30C) was mixed with 20 μL of 2 mM $Ag^+$ at 37°C for 2 h. The obtained mixture was further used to survey the effect of DNA structure on postshaping of AgNTs.

**Detection of S1 and TdT via DNA-guided postshaping of HRP-protected AgNTs.**

To quantify the activity of S1, 5'-phosphomononucleotide was first generated with poly(30C) and S1. In detail, different concentrations of S1 (2 μL, from 0 to 20 U/μL), $Zn^{2+}$ ions (4 μL, 10 mM), poly(30C) (20 μL, 10 μM), and 14 μL of $H_2O$ were incubated at 37°C for 30 min. Then, the mixture was heated at 90°C for 5 min, and gradually cooled to room temperature. Then, the solution was mixed with 360 μL of AgNTs solutions for 70 min. During the process, the color of solution changed from green to blue. Finally, extinction spectra of the solution were recorded to quantify the activity of

S1. In order to quantify the activity of TdT, C-rich DNA was obtained with poly(10T), dCTP, and TdT. Different concentrations of TdT (20 μL, from 0 to 15 U/μL), dCTP (5 μL, 10 mM), poly(10T) (2 μL, 10 μM), $Co^{2+}$ (8 μL, 5mM) and 5 μL $H_2O$ were incubated at 37°C for 3 h. Then, the mixture was heated at 75°C for 20 min to inactivate the TdT. The other procedure was similar to that of S1 detection.

**Simulation of electric field distribution and electric field vectors.**

Theoretical calculations were performed by the boundary element methods, using the Matlab Toolbox of metallic nanoparticle boundary element method (MNPBEM).[S2] The different stages of etched AgNTs were set up by a triangular nanoprism with different curvature radius of rounded corners. The electric field distribution, electric field vectors and extinction spectra of AgNTs were calculated by solving the Maxwell equations under a planewave excitation. The dielectric environment of the surrounding media and the silver nanoplates were defined by a constant dielectric function with refractive index of 1.33 (water) and a tabulated dielectric function extracted from experimental data.[S3] The meshes of the AgNTs were optimized to achieve a consistent convergence result.

## 2. Absorption spectrum of $Ti(SO_4)_2$ solution mixed with the supernate of as-prepared AgNTs.

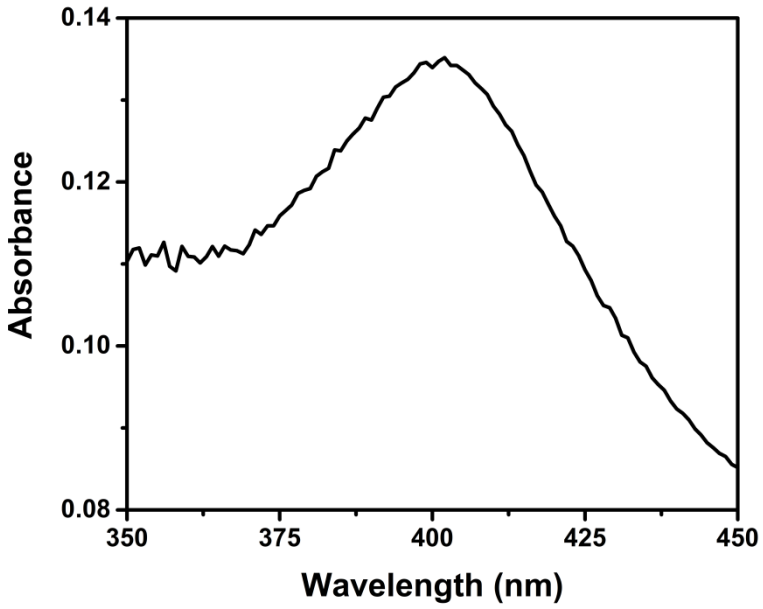


**Figure S1.** Absorption spectrum of $Ti(SO_4)_2$ solution mixed with the supernate of as-prepared AgNTs.

## 3. TEM and HAADF-STEM images of AgNTs.

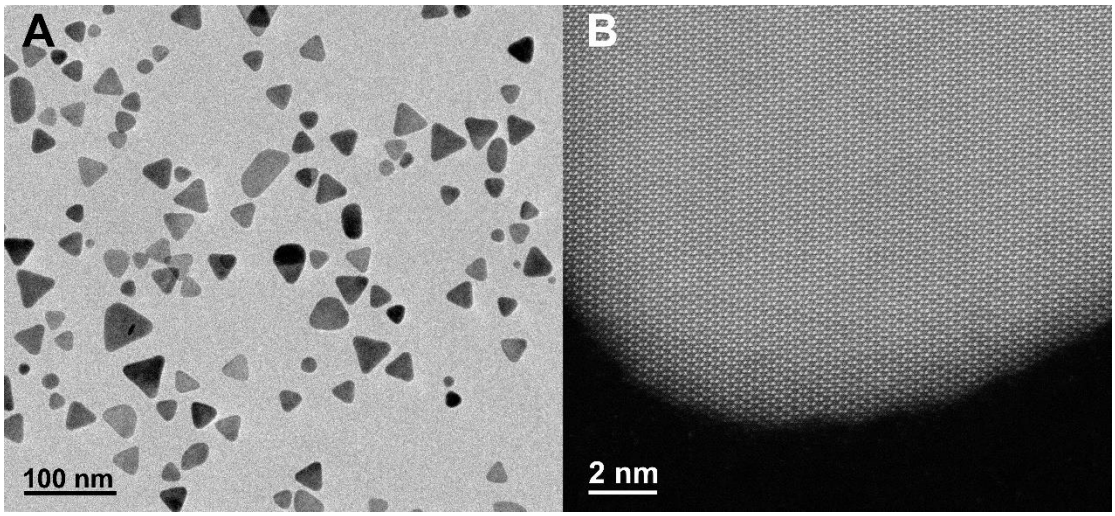


**Figure S2.** (A) TEM and (B) HAADF-STEM images of AgNTs.

## 4. Effect of different concentration of $H_2O_2$ on HRP-protected AgNTs.

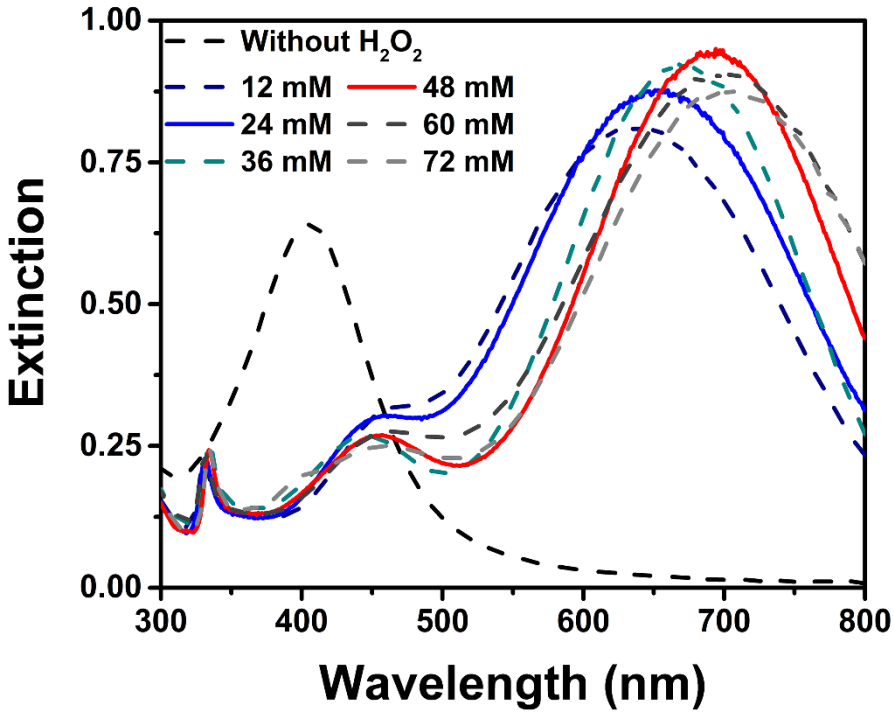


**Figure S3.** Extinction spectra of HRP-protected AgNTs obtained with the different concentrations of $H_2O_2$.

## 5. Crystal characterization of AgNTs and HRP-protected AgNTs.

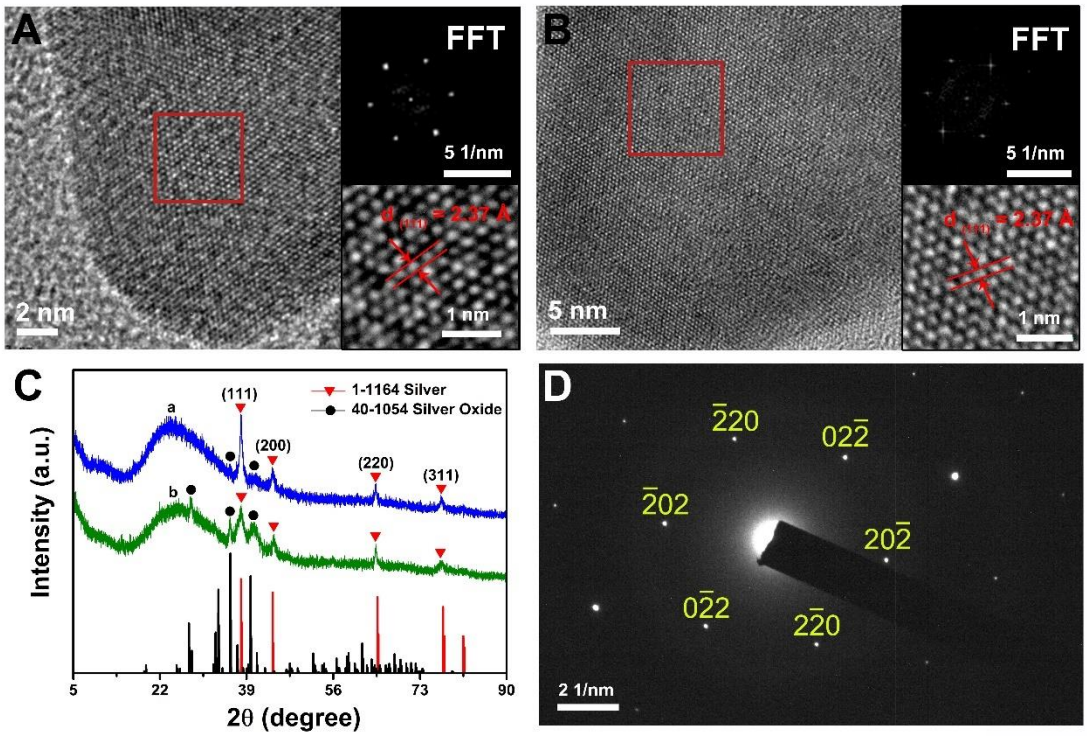


**Figure S4.** (A) HRTEM image of AgNTs. Insert: Fast fourier transformation (FFT) and inverse fast fourier transformation (IFFT) images of AgNTs. (B) HRTEM image of HRP-protected AgNTs. Insert: FFT and IFFT images of HRP-protected AgNTs. (C) The XRD patterns of a) AgNTs and b) HRP-protected AgNTs. (D) SAED pattern of the HRP-protected AgNTs.

## 6. Effect of different biomolecules on AgNTs.

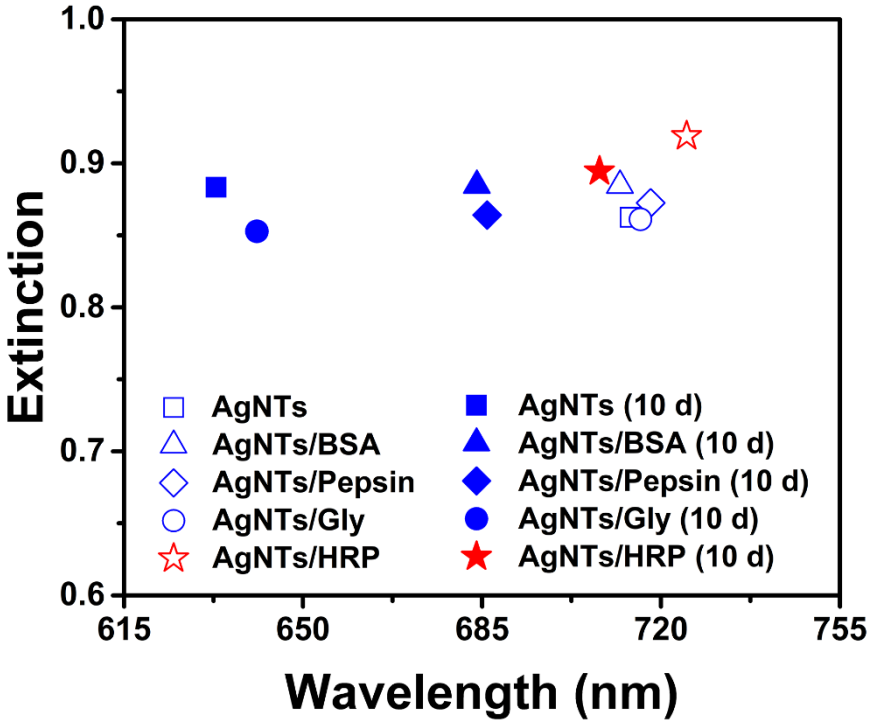


**Figure S5.** Effects of BSA, pepsin, Gly and HRP on stability of AgNTs.

## 7. Zeta potential results of HRP, AgNTs and HRP-protected AgNTs.

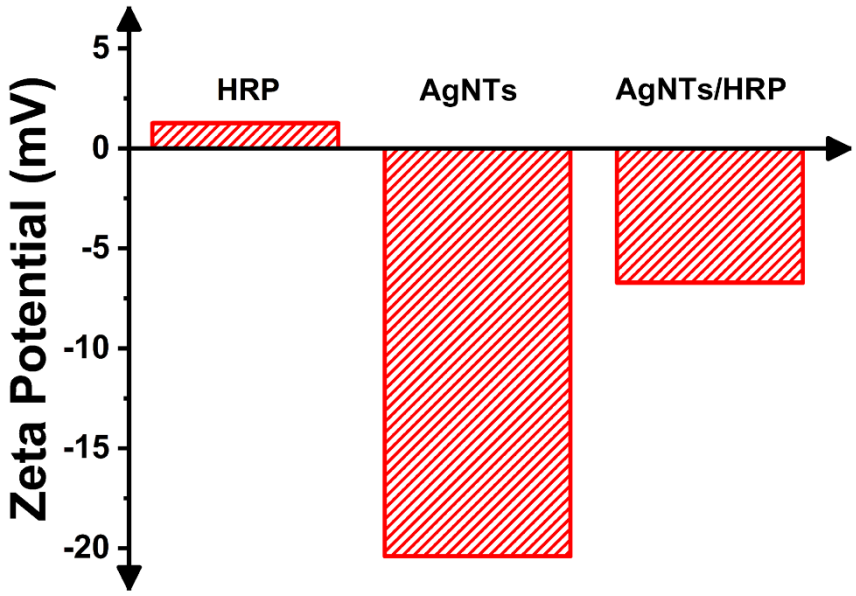


**Figure S6.** Zeta potential results of HRP, AgNTs and HRP-protected AgNTs.

## 8. SEM images of HRP and HRP-protected AgNTs as well as STEM images of HRP-protected AgNTs.

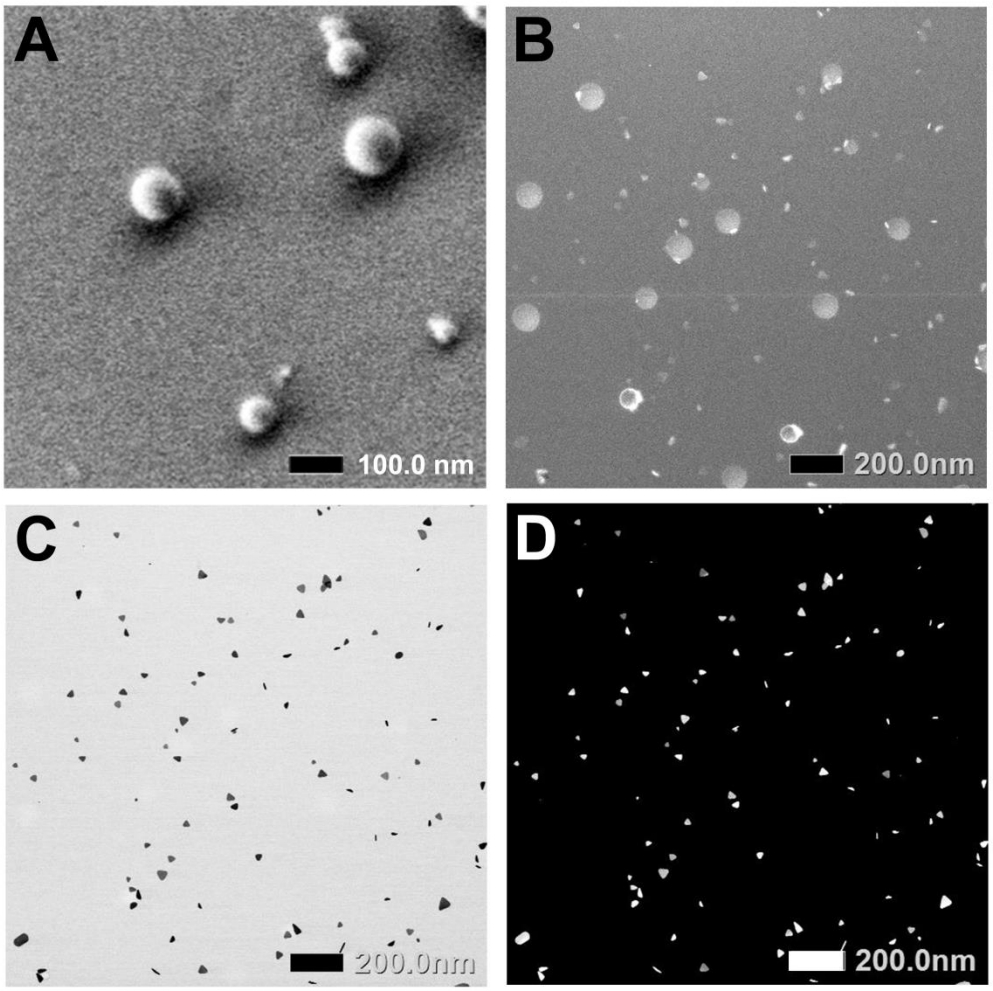


**Figure S7.** SEM images of (A) HRP and (B) HRP-protected AgNTs. (C) Bright-field and (D) dark-field STEM images of HRP-protected AgNTs.

## 9. Stability of AgNTs and HRP-protected AgNTs.

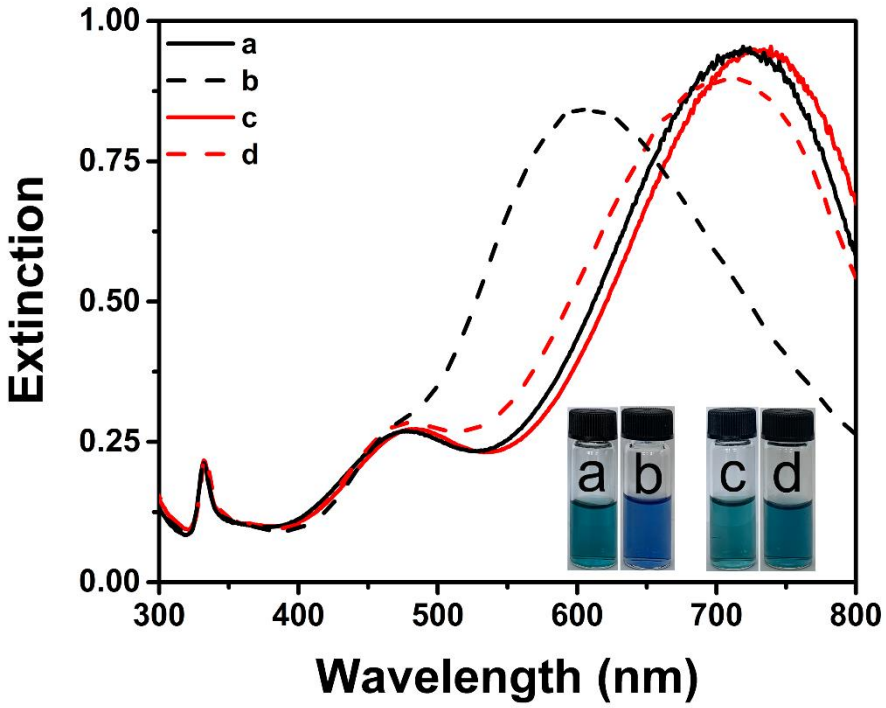


**Figure S8**. Extinction spectra of (a) as-prepared AgNTs, (b) AgNTs stayed at room temperature for 20 d, (c) as-prepared HRP-protected AgNTs, and (d) HRP-protected AgNTs stayed at room temperature for 20 d. Insert: The photographs of corresponding solutions.

## 10. Optimization of the protection effect of HRP on AgNTs.

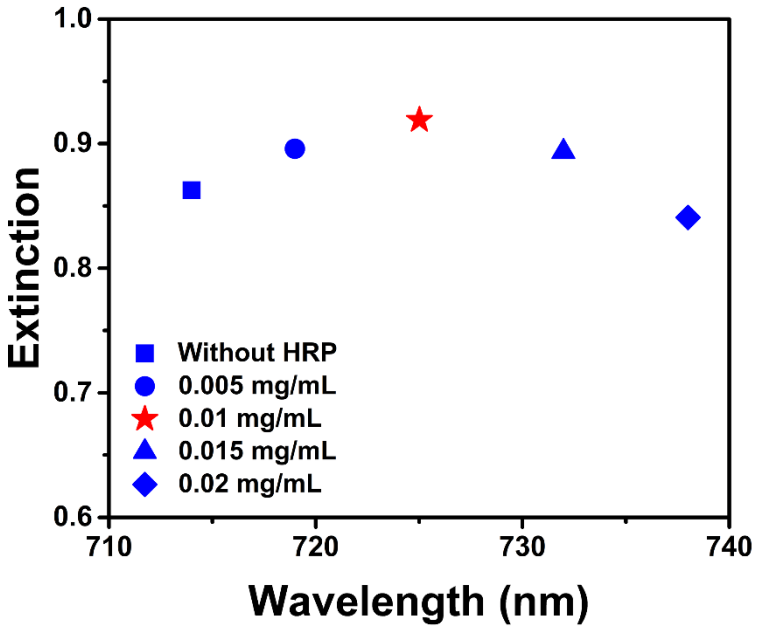


**Figure S9.** Extinction peak value and wavelength of AgNTs in the presence of different concentrations of HRP.

## 11. Zoomed out TEM images of HRP-protected AgNTs with poly(30C).

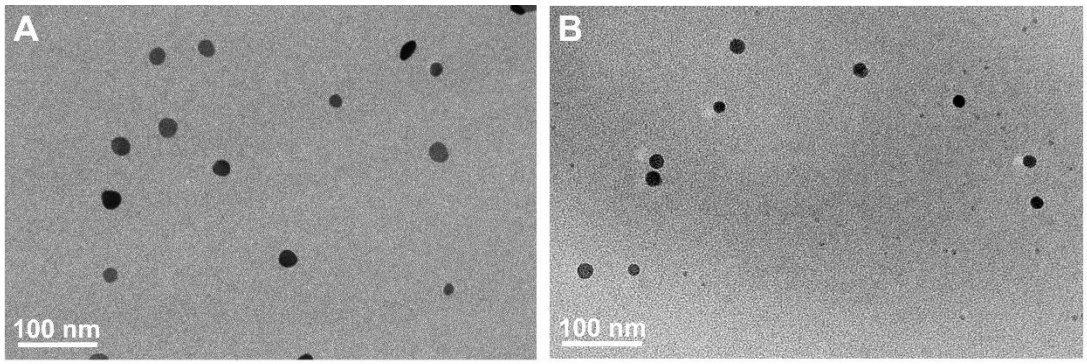


**Figure S10.** Zoomed out TEM images of HRP-protected AgNTs and poly(30C) for (A) 70 min and (B) 10 d.

## 12. Evolution process of HRP-protected AgNTs etched by poly(30C).

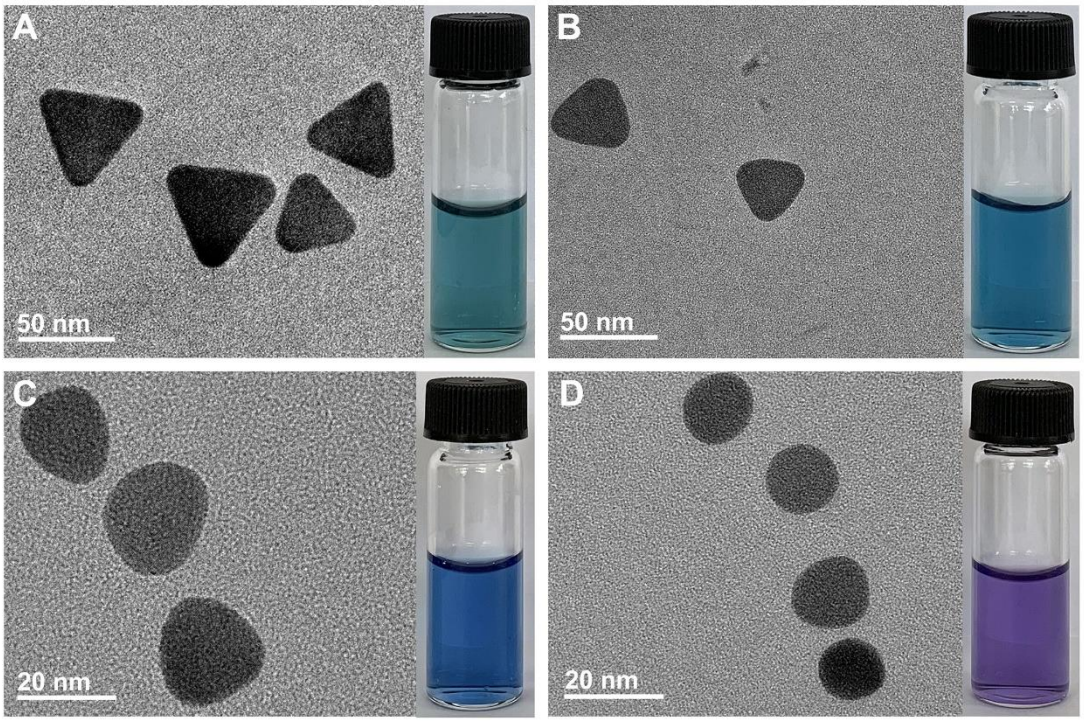


**Figure S11.** TEM images and photographs of HRP-protected AgNTs and poly(30C) with incubation time of (A) 0 min, (B) 10 min, (C) 70 min and (D) 10 d.

At the first 10 min, corners of AgNTs are etched by poly(30C), producing passivated AgNTs (Figure S11B). Then, edges of AgNTs are etched, generating irregular nanodisks (Figure S11C). More than 70 min later, the shaping process becomes slow, and AgNTs evolve into nanodisks (Figure S11D).

## 13. Time-dependent extinction spectra of HRP-protected AgNTs and poly(30C).

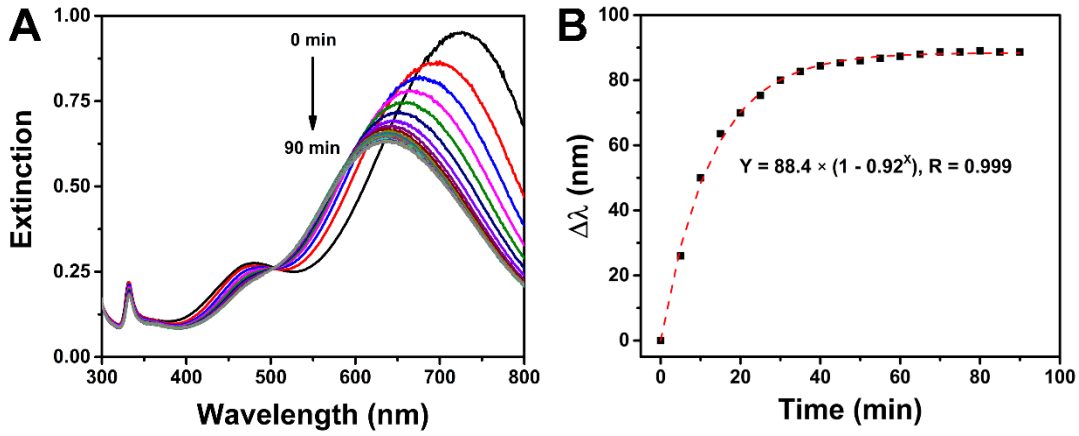


**Figure S12.** (A) Representative time-dependent extinction spectra of the HRP-protected AgNTs and poly(30C) with different incubation time (from top to bottom: 0, 5, 10, 15, 20, 25, 30, 35, 40, 45, 50, 55, 60, 65, 70, 75, 80, 85, 90 min, respectively). (B) Plot of shift of extinction peak (Δλ) as a function of incubation time.

## 14. Dependence of extinction wavelength on edge length of AgNTs.

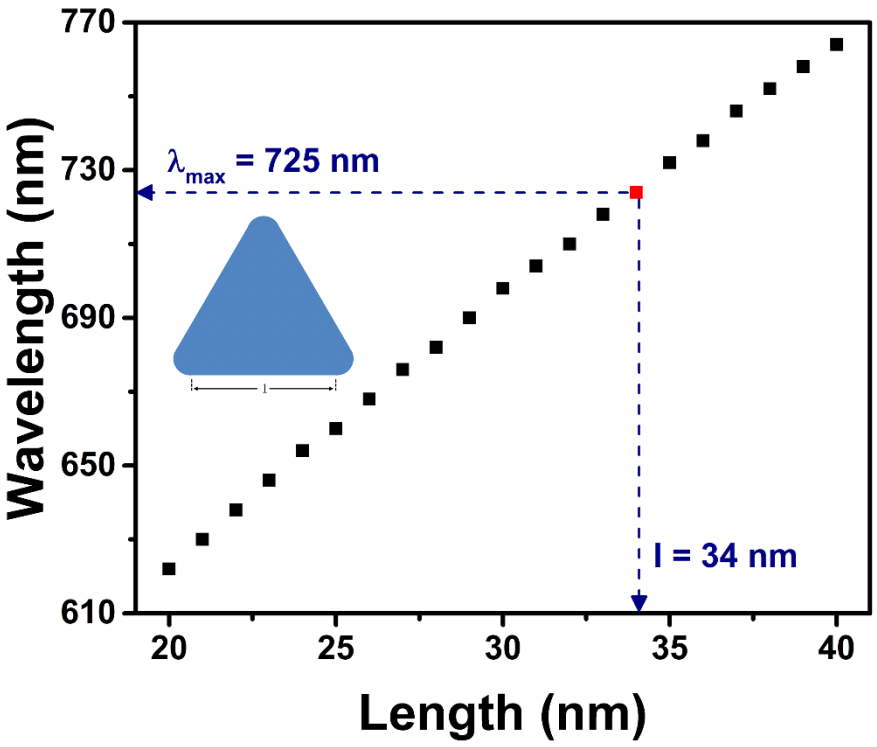


**Figure S13.** Dependence of extinction wavelength on edge length of AgNTs.

## 15. Construction of a relationship between $r_0$ and incubation time

Relationship between $r_0$ and incubation time is constructed based on the data of Figure 2H, Figure S12 and S13. Taking $r_0$ = 5 nm as an example, the extinction wavelength of AgNTs with $r_0$ = 5 nm is 707 nm (Figure 2H). Since extinction wavelength of original AgNTs is 725 nm (Figure S13), shift of extinction peak ($\Delta\lambda$) is calculated to be 18 nm. As shown in Figure S12, $\Delta\lambda$ (Y) and incubation time (X) are consistent with the calibration equation of $Y = 88.4 \times (1 - 0.93^X)$. According to the equation, X is 3 min in the case of Y = 18 nm. On a basis of the above procedure, incubation time for different $r_0$ can be deduced.

## 16. Effect of C-rich DNA on etching of HRP-protected AgNTs.

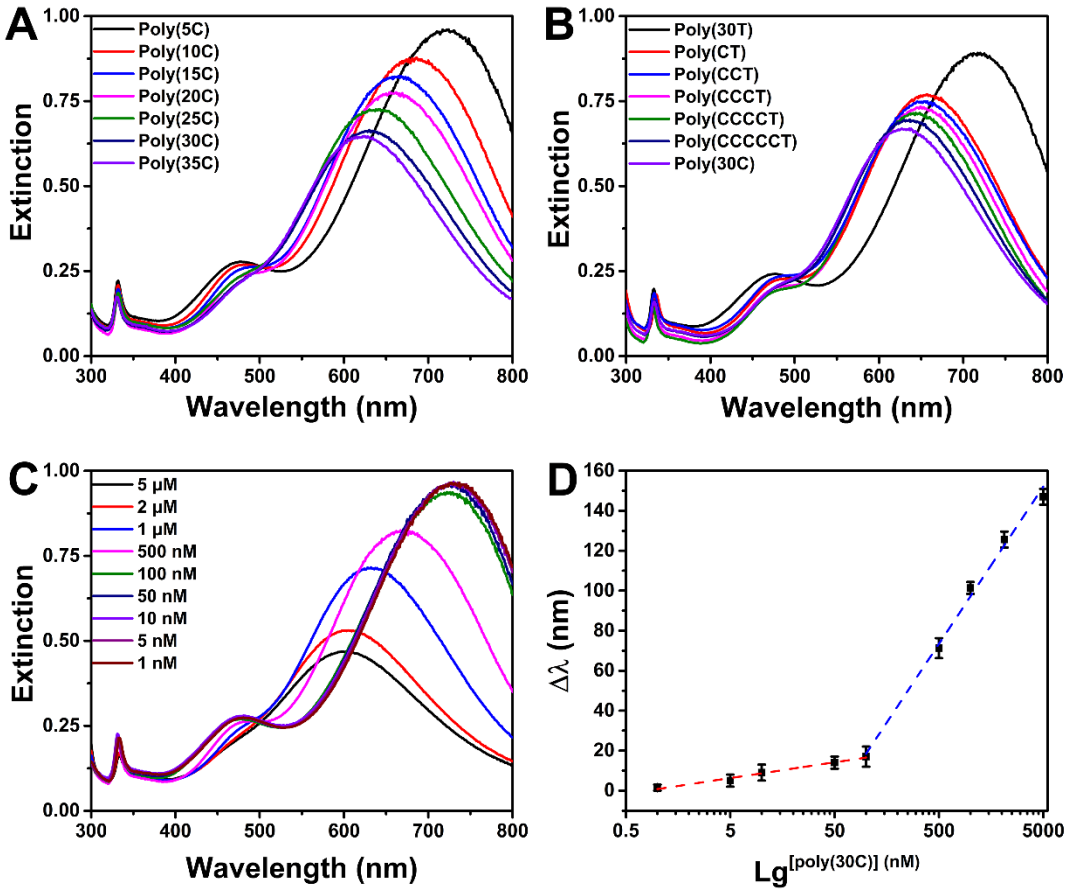


**Figure S14.** (A) Extinction spectra of HRP-protected AgNTs and poly(5C), poly(10C), poly(15C), poly(20C), poly(25C), poly(25C) and poly(35C). (B) Extinction spectra of HRP-protected AgNTs and poly(30T), poly(CT), poly(CCT), poly(CCCT), poly(CCCCT), poly(CCCCCT) and poly(30C). (C) Extinction spectra of HRP-protected AgNTs and different concentrations of poly(30C). (D) Plot of Δλ as a function of concentration of poly(30C).

## 17. XPS spectra of HRP-protected AgNTs and poly(30C) with different incubation time.

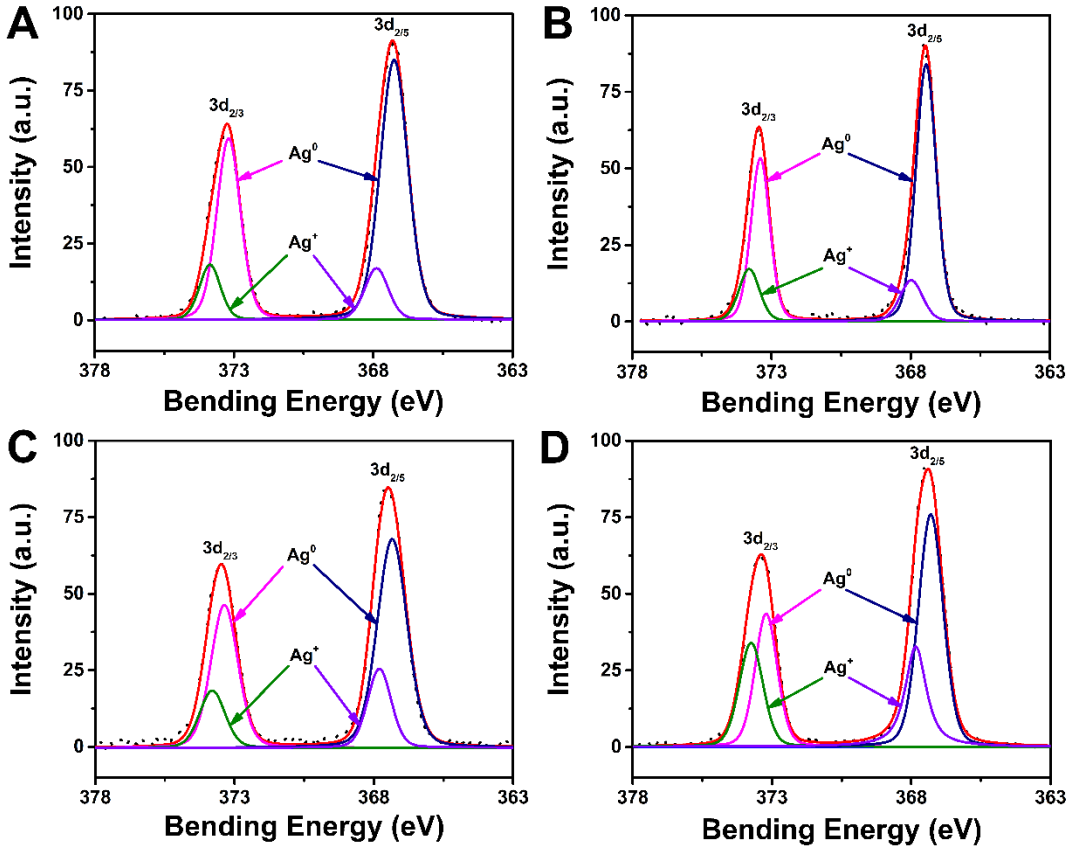


**Figure S15.** (A) XPS spectra of HRP-protected AgNTs for the element of Ag 3d. The ratio of $Ag^0$ and $Ag^+$ is 83% : 17%. (B) XPS spectra of HRP-protected AgNTs and poly(30C) with incubation time of 30 min for the element of Ag 3d. The ratio of $Ag^0$ and $Ag^+$ is 80.6% : 19.4%. (C) XPS spectra of HRP-protected AgNTs with incubation time of 1 h for the element of Ag 3d. The ratio of $Ag^0$ and $Ag^+$ is 75.3% : 24.7%. (D) XPS spectra of HRP-protected AgNTs with incubation time of 2 h for the element of Ag 3d. The ratio of $Ag^0$ and $Ag^+$ is 61.9% : 38.1%.

## 18. Effect of various surfactants on DNA-guided postshaping.

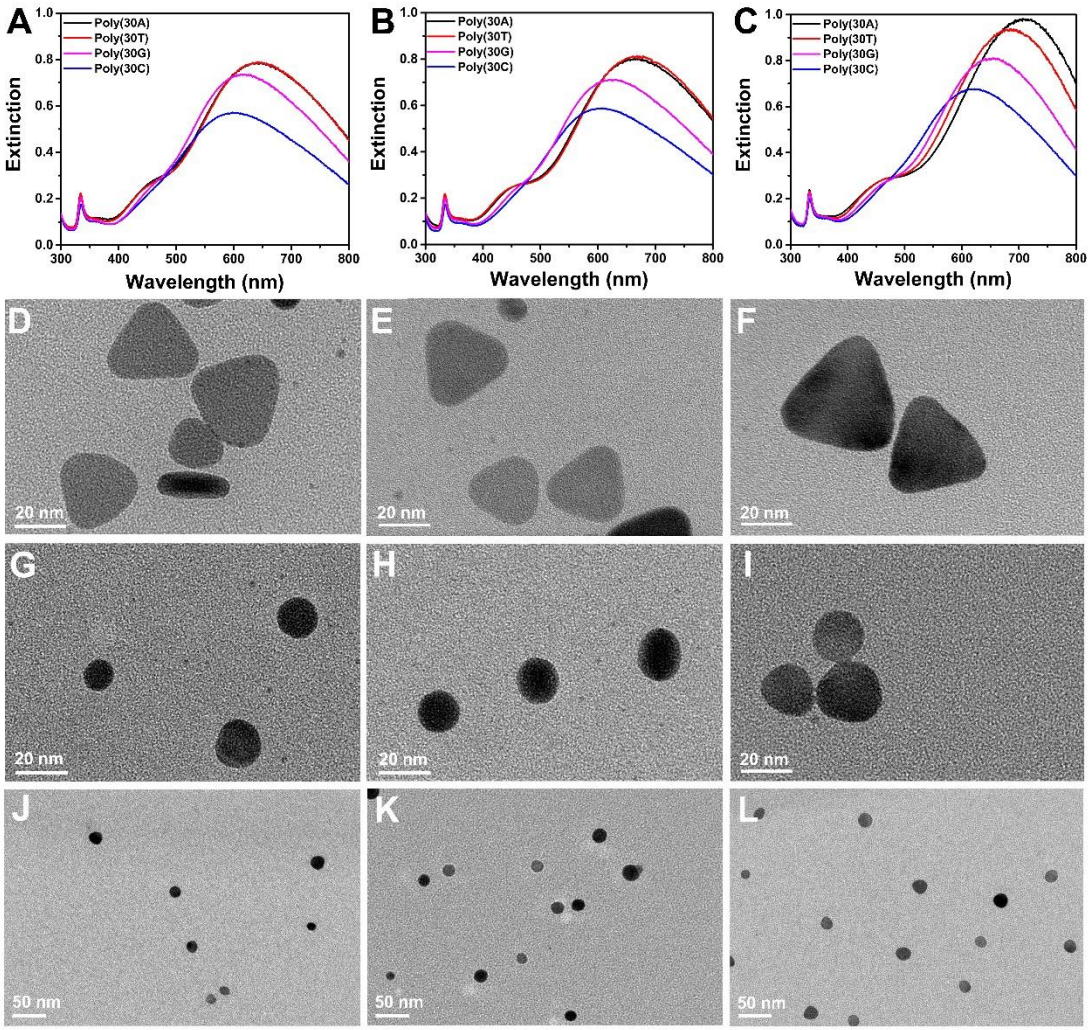


**Figure S16.** The extinction spectra of (A) ethanol-capped HRP-protected AgNTs, (B) EG-capped HRP-protected AgNTs, and (C) PEG-capped HRP-protected AgNTs with poly(30A), poly(30T), poly(30C) and poly(30G). TEM images of (D) ethanol-capped HRP-protected AgNTs, (E) EG-capped HRP-protected AgNTs, and (F) PEG-capped HRP-protected AgNTs. TEM images of (G) ethanol-capped HRP-protected AgNTs with poly(30C), (H) EG-capped HRP-protected AgNTs with poly(30C), and (I) PEG-capped HRP-protected AgNTs with poly(30C). Zoomed out TEM images of (J) ethanol-capped HRP-protected AgNTs with poly(30C), (K) EG-capped HRP-protected AgNTs with poly(30C), and (L) PEG-capped HRP-protected AgNTs with poly(30C).

## 19. Dependence of extinction spectra of HRP-protected AgNTs on different activities of S1 and TdT.

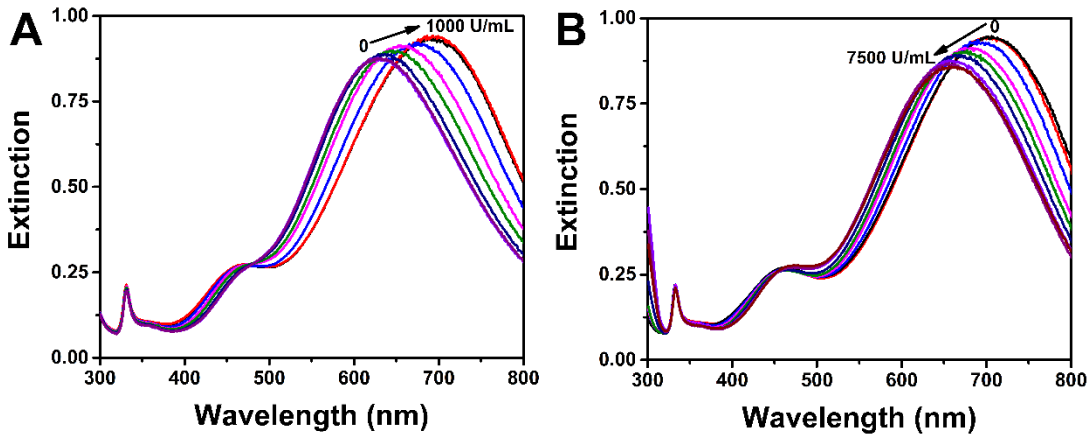


**Figure S17**. (A) Extinction spectra of HRP-protected AgNTs and poly(30C) treated with different concentrations of S1. (B) Extinction spectra of HRP-protected AgNTs and poly(10T) treated with different activities of TdT.

As shown in Figure 4B and Figure S17A, $\Delta\lambda$ is correlated with the activity of S1 ([S1]) from 0.005 to 500 U/mL. The detection limit of this method is 0.003 U/mL, and the regression equation is $\Delta\lambda = 39.4 - 13.7\lg^{[S1]}$ ($R = 0.996$). Activity of TdT ([TdT]) is measured in a linear range from 5 to 5000 U/mL with a detection limit of 2.6 U/mL (Figure 4C and S17B). The regression equation is $\Delta\lambda = 17.8\lg^{[TdT]} - 11.1$ ($R = 0.998$).

## 20. Comparison of analytical performances of different S1 biosensors.

**Table S2.** Comparison of analytical performances of different S1 biosensors.

| **Method** | **Detection limit (U/mL)** | **Linear range (U/mL)** | **Cost** | **DNA modification** | **Ref.** |
|---|---|---|---|---|---|
| Photoluminescence | 0.0014 | 0.003 - 0.017 | Medium | Not required | S4 |
| Electrochemistry | 0.27 | 1 - 10 | Low | Not required | S5 |
| Fluorescence | 0.14 | 2 - 70 | High | Required | S6 |
| Fluorescence | 0.3 | 1 - 5 | Low | Not required | S7 |
| Colorimetry | $5.9 \times 10^{-4}$ | $1.0 \times 10^{-3}$ - 1 | High | Required | S8 |
| Colorimetry | 4.3 | 4.3 - 30 | Medium | Not required | S9 |
| Colorimetry | $3.0 \times 10^{-3}$ | $5.0 \times 10^{-3}$ - 500 | Low | Not required | This work |

## 21. Comparison of analytical performances of different TdT biosensors.

**Table S3.** Comparison of analytical performances of different TdT biosensors.

| **Method** | **Detection limit (U/mL)** | **Linear range (U/mL)** | **Cost** | **DNA modification** | **Ref.** |
|---|---|---|---|---|---|
| Luminescence | 0.25 | 0 - 8 | Low | Not required | S10 |
| Electrochemistry | 0.08 | 0.4 - 90 | Low | Not required | S11 |
| Electrochemistry | 0.83 | 3.3 - 813 | Medium | Not required | S12 |
| Fluorescence | $6.62 \times 10^{-4}$ | $1.96 \times 10^{-3}$ - 1.96 | Medium | Not required | S13 |
| Fluorescence | $1.0 \times 10^{-3}$ | $1.0 \times 10^{-3}$ - 1 | High | Required | S14 |
| Colorimetry | 3.94 | 30 - 400 | Low | Not required | S15 |
| Colorimetry | 2.6 | 5 - 5000 | Low | Not required | This work |

## 22. Selectivity of the two etching-based methods.

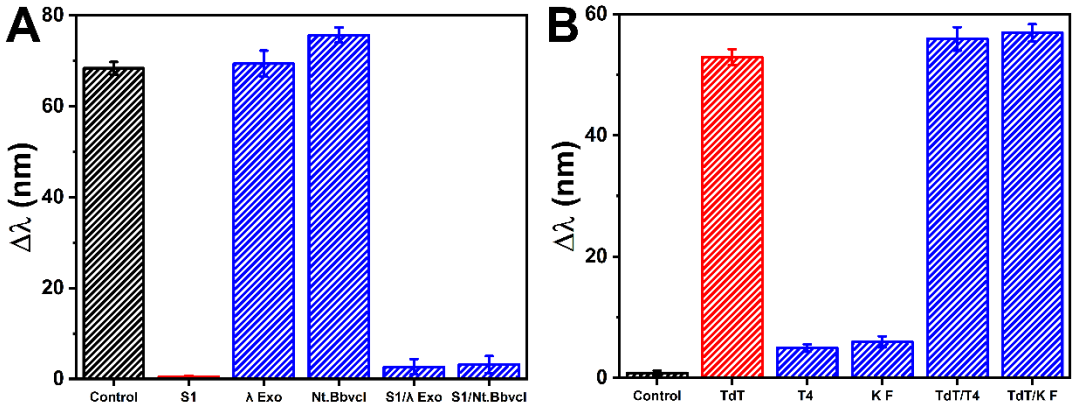


**Figure S18.** (A) Comparison of Δλ caused by S1, λ Exo, Nt.BbvcI, S1 and λ Exo, S1 and Nt.BbvcI. The activity of enzymes used in this assay is 20 U. (B) Comparison of Δλ caused by TdT, T4, K F, TdT and T4, TdT and K F. The activity of enzymes used in this assay is 200 U.

## 23. References.

(S1) Zhang, Q.; Li, N.; Goebl, J.; Lu, Z.; Yin, Y. A systematic study of the synthesis of silver nanoplates: is citrate a "magic" reagent? *J. Am. Chem. Soc.* **2011,** *133*, 18931-18939.

(S2) Hohenester, U.; Trügler, A. MNPBEM - A Matlab toolbox for the simulation of plasmonic nanoparticles. *Comput. Phys. Commun.* **2012**, *183*, 370-381.

(S3) Johnson, P. B.; Christy, R. W. Optical constants of the noble metals. *Phys. Rev. B* **1972,** *6*, 4370-4379.

(S4) Yuan, P.; Ma, R.; Gao, N.; Garai, M.; Xu, Q. H. Plasmon coupling-enhanced two-photon photoluminescence of Au@Ag core-shell nanoparticles and applications in the nuclease assay. *Nanoscale* **2015,** *7*, 10233-10239.

(S5) Ding, J.; Qin, W. Potentiometric sensing of nuclease activities and oxidative damage of single-stranded DNA using a polycation-sensitive membrane electrode. *Biosens. Bioelectron.* **2013,** *47*, 559-565.

(S6) Xiao, Y.; Shu, F.; Wong, K. Y.; Liu, Z. Forster resonance energy transfer-based biosensing platform with ultrasmall silver nanoclusters as energy acceptors. *Anal. Chem.* **2013,** *85*, 8493-849

(S7) Hu, R.; Liu, Y. R.; Kong, R. M.; Donovan, M. J.; Zhang, X. B.; Tan, W.; Shen, G. L.; Yu, R. Q. Double-strand DNA-templated formation of copper nanoparticles as fluorescent probe for label free nuclease enzyme detection. *Biosens. Bioelectron.* **2013,** *42*, 31-35.

(S8) Wang, Z.; Zhao, J.; Bao, J.; Dai, Z. Construction of metal-ion-free G-quadruplex-hemin DNAzyme and its application in S1 nuclease detection. *ACS Appl. Mater. Interfaces* **2016,** *8*, 827-833.

(S9) Cao, R.; Li, B.; Zhang, Y.; Zhang, Z. Naked-eye sensitive detection of nuclease activity using positively-charged gold nanoparticles as colorimetric probes. *Chem. Commun.* **2011,** *47*, 12301-12303.

(S10) Lu, L.; Wang, M.; Liu, L. J.; Wong, C. Y.; Leung, C. H.; Ma, D. L. A luminescence switch-on probe for terminal deoxynucleotidyl transferase (TdT) activity detection by using an iridium(III)-based i-motif probe. *Chem. Commun.* **2015,** *51*, 9953-9956.

(S11) Hu, Y.; Zhang, Q.; Guo, Z.; Wang, S.; Du, C.; Zhai, C. In situ grown DNA nanotail-templated silver nanoclusters enabling label-free electrochemical sensing of terminal deoxynucleotidyl transferase activity. *Biosens. Bioelectron.* **2017,** *98*, 91-99.

(S12) Du, C.; Shang, A.; Shang, M.; Zhang, J.; Song, W. Surface-functionalized $MoS_2$ ultrathin nanosheets for electrochemical monitoring terminal deoxynucleotidyl transferase activity based on in-situ polymerized DNA. *Sens. Actuators, B* **2018,** *277*, 297-305.

(S13) Liu, X.; Wang, H.; Deng, K.; Kwee, S.; Huang, H.; Tang, L. Single primer based multisite strand displacement reaction amplification strategy for rapid detection of terminal deoxynucleotidyl transferase activity. *Anal. Chem.* **2019,** *91*, 7482-7486.

(S14) Wang, L. J.; Luo, M. L.; Zhang, Q.; Tang, B.; Zhang, C. Y. Single quantum dot-based nanosensor for rapid and sensitive detection of terminal deoxynucleotidyl transferase. *Chem. Commun.* **2017,** *53*, 11016-11019.

(S15) Liu, Z.; Li, W.; Nie, Z.; Peng, F.; Huang, Y.; Yao, S. Randomly arrayed G-quadruplexes for label-free and real-time assay of enzyme activity. *Chem. Commun.* **2014,** *50*, 6875-6878.